Journal of Neurochemistry
Lippincott Williams & Wilkins, Inc., Philadelphia

The A-Type Potassium Channel Kv4.2 Is a Substrate for the Mitogen-Activated Protein Kinase ERK

J. Paige Adams, *Anne E. Anderson, Andrew W. Varga, Kelly T. Dineley, †Richard G. Cook, Paul J. Pfaffinger, and J. David Sweatt

*Division of Neuroscience, *Departments of Pediatrics and Neurology, and †Department of Microbiology and Immunology, Baylor College of Medicine, Houston, Texas, U.S.A.*

Abstract: The mitogen-activated protein kinase ERK has recently become a focus of studies of synaptic plasticity and learning and memory. Due to the prominent role of potassium channels in regulating the electrical properties of membranes, modulation of these channels by ERK could play an important role in mediating learning-related synaptic plasticity in the CNS. Kv4.2 is a Shal-type potassium channel that passes an A-type current and is localized to dendrites and cell bodies in the hippocampus. The sequence of Kv4.2 contains several consensus sites for ERK phosphorylation. In the present studies, we tested the hypothesis that Kv4.2 is an ERK substrate. We determined that the Kv4.2 C-terminal cytoplasmic domain is an effective ERK2 substrate, and that it is phosphorylated at three sites: Thr^{602}, Thr^{607}, and Ser^{616}. We used this information to develop antibodies that recognize Kv4.2 phosphorylated by ERK2. One of our phospho-site-selective antibodies was generated using a triply phosphorylated peptide as the antigen. We determined that this antibody recognizes ERK-phosphorylated Kv4.2 in COS-7 cells transfected with Kv4.2 and native ERK-phosphorylated Kv4.2 in the rat hippocampus. These observations indicate that Kv4.2 is a substrate for ERK in vitro and in vivo, and suggest that ERK may regulate potassium-channel function by direct phosphorylation of the pore-forming α subunit. **Key Words:** Suprasynaptic plasticity—Hippocampus—Phosphorylation—Long-term potentiation—Epilepsy.
J. Neurochem. **75,** 2277–2287 (2000).

Although typically studied in the context of the regulation of cell division and differentiation, the mitogen-activated protein kinase (MAPK) cascade has been implicated recently as a player in the regulation of synaptic strength (Impey et al., 1999). In the mammalian CNS, the MAPK cascade has been found to play an important role in hippocampal long-term potentiation (LTP), a candidate cellular mechanism for learning and memory. In particular, the MAPK ERK2 (extracellular signal-regulated kinase 2) is activated in area CA1 of the hippocampus following LTP-inducing high-frequency stimulation; in addition, blockade of ERK activation inhibits induction of stable LTP (English and Sweatt, 1996, 1997). Moreover, ERK has been shown recently to be involved in several forms of mammalian learning and memory, including fear conditioning (Atkins et al., 1998; Schafe et al., 1999), conditioned taste aversion (Berman et al., 1998), and spatial learning (Blum et al., 1999; Selcher et al., 1999).

The substrates for ERK phosphorylation during the induction of LTP are largely unknown. The modulation of potassium (K^+) channels by ERK is a particularly intriguing possibility in the context of LTP induction, due to the ability of K^+ channels to regulate membrane electrical responsiveness. It has been discovered recently that voltage-dependent K^+ channels that flux an A-type current (I_A) in the dendrites of hippocampal pyramidal neurons play a critical role in shaping the electrical responses of these neurons (Hoffman et al., 1997). One particular A-type K^+-channel subunit protein, the Shal-type channel Kv4.2, has been localized to somas and distal dendrites in area CA1 of the rat hippocampus, including sites of synaptic contacts (Sheng et al., 1992; Maletic-Savatic et al., 1995; Alonso and Widmer, 1997). Kv4.2 subunits most likely form at least part of dendritic A-type channels in area CA1 pyramidal neurons (Cassell and McLachlan, 1986; Baldwin et al., 1991). Indeed, using antisense hybrid arrest in oocytes transfected with rat brain mRNA, it has been found that I_A is eliminated almost completely by targeting Kv4.2 channels (Serodio et al., 1994). In hippocampal CA1 pyramidal cells, sin-

Received May 11, 2000; revised manuscript received July 26, 2000; accepted July 27, 2000.

Address correspondence and reprint requests to Dr. J. D. Sweatt at Division of Neuroscience, Baylor College of Medicine, One Baylor Plaza, Houston, TX 77030, U.S.A. E-mail: jsweatt@bcm.tmc.edu

Abbreviations used: CPM, counts per minute; EGF, epidermal growth factor; ERK, extracellular signal-regulated kinase; GST, glutathione *S*-transferase; I_A, A-type current; LTP, long-term potentiation; MAPK, mitogen-activated protein kinase; MEK, mitogen-activated protein kinase kinase; PBS, phosphate-buffered saline; PKA, cyclic AMP-dependent protein kinase; PKC, protein kinase C; RT, room temperature; SDS, sodium dodecyl sulfate.

gle-cell RT-PCR has been used to confirm the importance of Kv4.2 in these neurons (Martina et al., 1998).

Small changes in the gating properties of the dendritic A-type channel have large effects on hippocampal area CA1 neuron electrical properties. For example, the modulation of dendritic I_A in area CA1 by activation of protein kinase C (PKC) or the cyclic AMP-dependent protein kinase (PKA) cascade results in an increase in the amplitude of back-propagating action potentials into the distal dendrites (Hoffman and Johnston, 1998). ERK is also present in the same subcellular compartments as Kv4.2 (Fiore et al., 1993; Lev et al., 1995), and examination of the Kv4.2 amino acid sequence reveals several potential ERK phosphorylation sites.

Here, we examined the phosphorylation of Kv4.2 by ERK. We determined that the C-terminus of Kv4.2 is a substrate for ERK2 in vitro, and we used direct amino acid sequencing to determine that ERK phosphorylates Kv4.2 at three sites: Thr^{602}, Thr^{607}, and Ser^{616}. We generated antibodies against a peptide containing all three phospho-sites and peptides containing each single phospho-site. Characterization of these antibodies reveals that they are selective for their antigen and that they are phospho-selective. Development of these antibodies provides a tool with which to examine the phosphorylation of Kv4.2 by ERK in native cells. For example, we determined that the antibody developed against the triply phosphorylated peptide recognizes phospho-Kv4.2 in COS-7 cells transfected with Kv4.2, as well as in the rat hippocampus. Taken together, our results provide strong evidence that Kv4.2 is an ERK substrate in vitro and in vivo.

EXPERIMENTAL PROCEDURES

Bacterial recombinant protein expression

The expression and purification of the N- and C-terminus glutathione *S*-transferase (GST) fusion proteins were performed as previously described (Anderson et al., 2000). In brief, fusion proteins consisting of the N-terminus (amino acids 1–133; see Fig. 1) or the C-terminus (amino acids 411–630) of Kv4.2 linked to GST were expressed in *E. coli* and then solubilized with 1.5% *N*-laurylsarcosine. The fusion proteins were purified using glutathione affinity absorption. Unless otherwise indicated, the fusion proteins were left on the beads for subsequent experiments.

ERK2 phosphorylation of Kv4.2 N- and C-terminus GST-fusion proteins

These reactions were performed in a final volume of 25 μl. The fusion proteins were incubated for 1 h, unless otherwise indicated, at 34°C with 15 μCi of [γ-^{32}P]ATP per reaction in the presence of activated ERK2, HEPES buffer (in m*M*: 25 HEPES, 0.5 EDTA, 0.5 EGTA, 1 $Na_4P_2O_7$, 10 μg/ml aprotinin, 10 μg/ml leupeptin), 10 m*M* $MgCl_2$, and 100 μ*M* ATP. The reaction was stopped with sample buffer [in m*M*: 30 Tris-HCl, pH 6.8, 200 dithiothreitol, 40% glycerol, 8% sodium dodecyl sulfate (SDS), 0.04 mg/ml bromophenol blue], and the samples were boiled for 5 min. The fusion proteins were separated using 12.5 or 15% SDS-polyacrylamide gel electrophoresis and visualized by Coomassie Blue staining. The phosphopeptides were identified by autoradiography. To quantify phosphorylation, autoradiographs were analyzed further by densitometry using NIH Image software. For time-course experiments, film exposure times were of short duration to insure nonsaturation of the film for long time-point samples.

Kinetic characterization of the Kv4.2 C-terminus phosphorylation sites

The C-terminus fusion protein was eluted off beads and then used as a substrate for activated ERK2. The reaction mixture (50 μl) contained 25 m*M* HEPES buffer, 250 ng of activated ERK2, and the GST-C-terminus fusion protein. Fusion protein concentrations ranging from 13.3 to 400 n*M* were used. The assay was started by the addition of 50 μ*M* ATP, 10 m*M* $MgCl_2$, and 5 μCi of [γ-^{32}P]ATP; the reaction mixture was incubated at 30°C for 30 min. As a control, parallel reactions using the ERK substrate myelin basic protein were performed. The reaction was stopped by spotting duplicate 20-μl aliquots of the reaction mixture onto Whatman 81 phosphocellulose filter papers and washing in 75 m*M* H_3PO_4. After a final wash in 99% methanol, the papers were dried and then immersed in Aquasol-2, and the radioactivity was counted. For each experimental condition, counts obtained from a reaction without substrate peptide were subtracted. The assays used to determine K_m and V_{max} values were linear with respect to time and linear with added kinase. In addition, $<$10% of the peptide substrate was converted to product.

Phosphopeptide mapping

These reactions were performed in a final volume of 500 μl. The GST-C-terminus fusion protein was incubated for 3 h at 34°C with 75 μCi of [γ-^{32}P]ATP per reaction in the presence of activated ERK2, HEPES buffer, 10 m*M* $MgCl_2$, and 100 μ*M* ATP. The reaction was stopped with sample buffer, and the samples were boiled for 5 min. The channel fusion proteins were separated by 12.5% SDS-polyacrylamide gel electrophoresis; thioglycolic acid was added to the running buffer to prevent blocking of the N-terminal end of the GST-C-terminal fusion protein. The channel fusion proteins were visualized by Coomassie Blue staining and excised from the gel. An in-gel Lys-C digestion was performed as previously described with minor modifications (Rosenfeld et al., 1992), and the peptides were separated by reverse-phase HPLC (Sweet et al., 1997). Absorption was monitored at 214, 254, and 280 nm, and counts per minute (CPM) were measured in each fraction as Cerenkov radiation. Automated amino acid sequence analysis was performed on fractions that contained peaks of radioactivity to identify the sequence of the phosphorylated peptides (Fredericks et al., 1996; Anderson et al., 2000). Phosphorylated amino acids in the peptide were determined by measuring the CPM released at each cycle of sequencing.

Antibody production

Synthetic peptides with the identified in vitro phosphorylation sites were produced by the Protein Core Facility at Baylor College of Medicine (see Fig. 4A). The peptides were synthesized with a cysteine attached to the C-terminal end of the peptide, so as to allow conjugation to the carrier protein keyhole limpet hemocyanin via *m*-maleimidobenzoyl-*N*-hydroxysuccinimide ester. The conjugates of the phosphopeptides were sent to a company specializing in the production of custom antibodies (Cocalico, Inc). After a preimmune blood was taken, the conjugates of the four phosphopeptides were each injected into two albino New Zealand rabbits with the adjuvant Titer-

max via intradermal injections. The animals were boosted with antigen several times.

Antibody purification

Each of the four antibodies was purified using Hi Trap NHS-activated affinity columns (Amersham–Pharmacia Biotech) according to the manufacturer's directions. Two milligrams of the appropriate antigen was loaded onto each column.

COS cell expression systems

COS-7 cells were cultured and transfected according to the DEAE-dextran method used by Dineley and Patrick (2000). In brief, 1×10^6 cells/150-mm culture dish were transfected with 8 μg of the appropriate cDNA in 10 ml of Dulbecco's modified Eagle's medium containing 1% antibiotics, 1% fetal bovine serum, 100 μM chloroquinone disulfate, and 0.04% DEAE-dextran. Following 4 h of incubation, cells were treated for 2 min with 10% dimethyl sulfoxide in phosphate-buffered saline (PBS; pH 7.5; in m*M*: 137 NaCl, 2.7 KCl, 4.3 Na_2HPO_4, 1.4 m*M* KH_2PO_4), followed by transfer to complete medium (Dulbecco's modified Eagle's medium, 10% fetal bovine serum, 1% antibiotics). Modulators of ERK activity were applied before harvesting in ice-cold PBS. After harvesting, the cells were collected via centrifugation for 10 min at 4°C at 3,000 rpm. The cell pellet was resuspended in 10% SDS with 200 m*M* dithiothreitol, 10 μg/ml aprotinin, leupeptin, and pepstatin, 100 μM phenylmethylsulfonyl fluoride, and 1 μM microcystin-LR; subsequently, 4× sample buffer containing 200 m*M* dithiothreitol was added. Following a brief sonication, the cellular proteins were loaded onto 10% SDS-polyacrylamide gels and resolved by standard electrophoresis (Bio-Rad minigel apparatus). Approximately 250,000 cells were loaded per lane.

Preparation of hippocampal slices

Hippocampal slices were prepared and maintained according to the method of Roberson et al. (1999). After a 60-min exposure to dimethyl sulfoxide (vehicle) or the MAPK kinase (MEK) inhibitor U0126, slices were immediately frozen on dry ice. The CA1 subregions were microdissected on dry ice and stored at −80°C until assayed. The resulting CA1 subregions from individual slices were sonicated according to Roberson et al. (1999). The sonicate was then centrifuged for 20 min at 4°C at 100,000 *g*; the pellet was resuspended as described above. Samples were loaded onto 10% SDS-polyacrylamide gels and resolved by standard electrophoresis. Approximately one CA1 subregion was loaded per lane.

Western blotting

Gels were blotted electrophoretically to Immobilon filter paper using a transfer tank maintained at 4°C. For samples of peptides, gels were transferred for 2 h at 600 mA; for samples of whole channels, gels were transferred overnight at 400 mA. Immobilon filters were blocked for 1 h at room temperature (RT) in a blocking solution containing 10 m*M* Tris-HCl, pH 7.5, 150 m*M* NaCl, 0.05% Tween 20, 5% milk, 0.01% thimerosal, and 1 μM microcystin-LR. The filters were incubated at RT sequentially with the purified antibody JPA170 (1:500) for 1 h, then with a horseradish peroxidase-conjugated secondary antibody (1:20,000) for 45 min. Blots were washed extensively in TTBS (50 m*M* Tris-HCl, pH 7.5, 150 m*M* NaCl, 0.05% Tween 20) after incubations with the primary and secondary antibodies. Blots were developed using enhanced chemiluminescence (ECL) or SuperSignal West Femto Maximum Sensitivity Substrate.

Immunohistochemistry

Adult C57BL/6 mice were anesthetized intraperitoneally with ketamine/xylazine and perfused transcardially with 10 ml of 0.9% NaCl followed by 50 ml of PBS, pH 7.4, containing 3% paraformaldehyde and 1% glutaraldehyde. The brains were cryoprotected in 30% sucrose in PBS for 24–48 h at 4°C until they sank, and then they were frozen and mounted for cryostat sectioning. Twenty-micrometer sections were cut and immediately thaw-mounted on Plus slides. Sections were incubated in 0.3% H_2O_2 in methanol for 30 min at RT and then blocked in PBS containing 0.2% Triton X-100 and 5% normal goat serum. After blocking medium was blotted from the slides, sections were incubated with a 1:100 dilution of primary antibody (JPA170) for 48 h in a humidified chamber at 4°C, followed by a 30-min incubation with a 1:200 dilution of goat anti-rabbit biotinylated secondary antibody at RT and a 30-min incubation with a 1:50 dilution of ABC reagent at RT. Staining was revealed with metal-enhanced diaminobenzidine. Blots were washed extensively in PBS containing 0.2% Triton X-100 after each incubation. Sections were then rinsed, cleared, and coverslipped using a xylene-based medium (Cytoseal 60 low-viscosity mounting medium).

Materials

Activated ERK2 was obtained from Stratagene. Hi Trap NHS-activated affinity columns and enhanced chemiluminescence were obtained from Amersham Pharmacia Biotech. The MEK inhibitor U0126 was provided by Promega (Adams et al., 1999). SuperSignal West Femtomax, ImmunoPure ABC peroxidase rabbit IgG staining kit, and metal-enhanced diaminobenzidine were obtained from Pierce. Cytoseal 60 was obtained from Stephens Scientific. Plus slides were obtained from VWR. Anti-Kv4.2 and anti-Kv4.3 antibodies were obtained from Alomone Labs. Anti-phospho-ERK was obtained from Upstate Biotechnology Inc. Horseradish peroxidase-conjugated secondary antibody was obtained from ICN. Microcystin-LR was obtained from BioMol. COS-7 cells were obtained from American Type Culture Collection. Kv4.2 and Kv4.3 cDNAs were kindly provided by L. Jan (Baldwin et al., 1991) and B. Rudy (Rudy et al., 1991).

RESULTS

MAPK phosphorylates the C-terminal domain, but not the N-terminal domain, of the Kv4.2 channel

The Shal family of K^+ channels, of which Kv4.2 is a member, is characterized by six transmembrane domains. The N- and C-termini are most likely intracellular, and thus accessible to cytoplasmic kinases. Previous studies have shown that members of the Shaker family of K^+ channels are regulated by phosphorylation of the N- and C-termini (Jonas and Kaczmarek, 1996). Inspection of the Kv4.2 channel sequence shows several potential ERK phosphorylation sites (Fig. 1). The minimal ERK consensus sequence is a serine or threonine followed by a proline (Kennelly and Krebs, 1991). One possible ERK phosphorylation site is located near the N-terminus; however, given the proposed topology for Kv channels, this site probably lies between the first and second transmembrane domains on the extracellular side of the membrane. Five other possible sites are located in the C-terminal domain, after the last transmembrane domain.

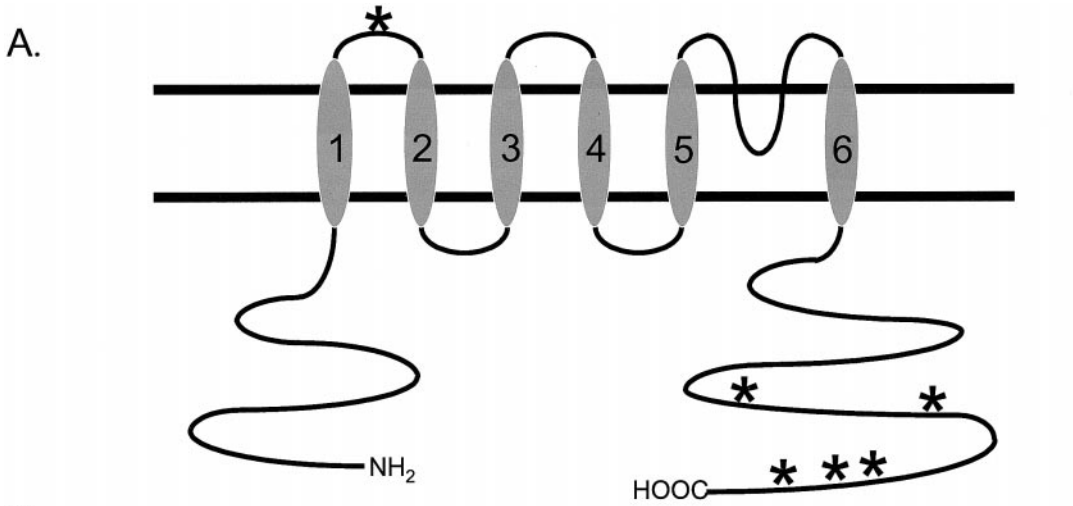

B.

MAAGVAAWLPFARAAAIGWMPVASGPMPAPPRQERKRTQDALIVLNVSGTRFQTWQDTLERYPDTLLGSSE
RDFFYHPETQQYFFDRDPDIFRHILNFYRTGKLHYPRHECISAYDEELAFFGLIPEIIGDCCYEEYKDRRR
ENAERLQDDADTDNTGESALPTMTARQRVWRAFENPHTSTMALVFYYVTGFFIAVSVIANVVETVPCG***SSP***
GHIKELPCGERYAVAFFCLDTACVMIFTVEYLLRLAAAPSRYRFVRSVMSIIDVVAILPYYIGLVMTDNED
VSGAFVTLRVFRVFRIFKFSRHSQGLRILGYTLKSCASELGFLLFSLTMAIIIFATVMFYAEKGSSASKFT
SIPAAFWYTIVTMTTLGYGDMVPKTIAGKIFGSICSLSGVLVIALPVPVIVSNFSRIYHQNQRADKRRAQK
KARLARIRAAKSGSANAYMQSKRNGLLSNQLQSSEDEPAFVSKSGSSFETQHHHLLHCLEKTTNHEFVDEQ
VFEESCMEVATVNRPSS***HSP***SLSSQQGVTSTCCSRRHKKSFRIPNANVSGSHRGSVQELSTIQIRCVE***RTP***
LSNSRSSLNAKMEECVKLNCEQPYVTTAIISI***PTP***PV***TTP***EGDDRP***ESP***EYSGGNIVRVSAL

FIG. 1. The Shal-type K^+ channel. **A:** Representative drawing of a mammalian voltage-gated K^+ channel, showing six transmembrane domains and the intracellular N- and C-terminal domains. Approximate locations of potential ERK phosphorylation sites are indicated by asterisks. **B:** The sequence of the Shal-type K^+ channel Kv4.2, with potential ERK phosphorylation sites italicized and underlined. One site is located toward the N-terminal portion of the channel. Five other sites are located on the intracellular C-terminal domain. Each of these sites conforms to the minimal ERK consensus sequence: a serine or threonine followed directly by a proline. The portions of the sequence used for N- and C-terminus fusion proteins are indicated with vertical bars.

Our examination of the phosphorylation of Kv4.2 by ERK began with an assessment of the phosphorylation of the cytoplasmic N- and C-terminal domains of Kv4.2 by ERK. Using N- or C-terminus GST-fusion proteins, we found that the C-terminus fusion protein was phosphorylated by activated ERK2, whereas the N-terminus fusion protein was not (Fig. 2A). As a control, GST was incubated with activated ERK2 and visualized by Coomassie staining and autoradiography. GST did not show phosphorylation by ERK2 (data not shown). This lack of phosphorylation confirms that ERK2 was not phosphorylating the GST attached to the C-terminal domain of Kv4.2. As a control for the reactions of ERK2 with the Kv4.2 N-terminus construct, myelin basic protein was incubated with ERK2 in a parallel reaction (data not shown). Myelin basic protein showed phosphorylation by ERK2, indicating that the ERK2 was active and capable of phosphorylating substrates. These in vitro results suggest that the C-terminal domain is a potential site for phosphorylation of the channel by ERK.

As a prelude to sequencing the sites in the Kv4.2 C-terminal domain construct phosphorylated by ERK, it was necessary to determine the time course of phosphorylation of this C-terminus construct. Phosphorylation of the C-terminus to saturating levels helps ensure that no possible phosphorylation sites are missed. The time course of the phosphorylation of the C-terminal domain of the Kv4.2 channel by ERK2 is shown in Fig. 2B. The results show that at 20 min, phosphorylation of the C-terminus fusion protein is still increasing; at 40 min, the C-terminus fusion protein phosphorylation has reached saturation levels. The data from this time course indicate that incubations of 1 h or more are sufficient for complete phosphorylation of the C-terminal domain by ERK2.

In preliminary kinetic characterizations, the Kv4.2 C-terminus construct was observed to be a very effective substrate for ERK2, with an estimated K_m of <60 nM and a V_{max} of 36 pmol/min/mg of protein (averages from two experiments performed in duplicate, under steady-state conditions; Fig. 2C). This compares favorably to the known ERK substrates microtubule-associated protein-2 (K_m = 56 nM), pp90RSK (K_m = 170 nM), and myelin basic protein (K_m = 254 nM) (Schanen and Landreth, 1992). It is interesting that, as has also been observed previously for other MAPK substrates (Erick-

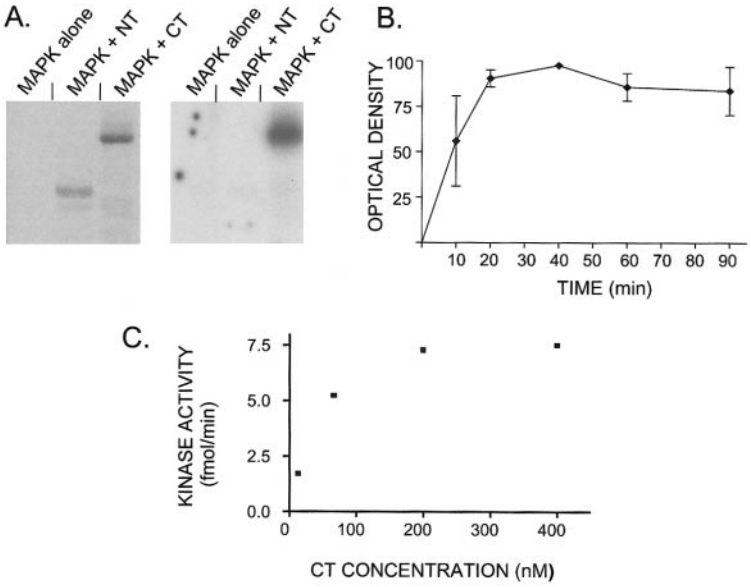

FIG. 2. Phosphorylation of Kv4.2 constructs by ERK2 in vitro. **A:** Representative Coomassie Blue-stained gel (**left**) and autoradiograph (**right**) showing that although both the N-terminus (NT) and C-terminus (CT) GST-fusion proteins are present, only the C-terminal domain is phosphorylated by ERK2. **B:** Time course of phosphorylation of the C-terminal domain of Kv4.2 by ERK2. By 40 min, the phosphorylation of the C-terminal domain reached saturation levels. Results show average normalized optical density of the autoradiograph band subtracted from background optical density for each time point examined. Error bars represent SEM. For each point, n = 3, except 40 min, where n = 2. **C:** Determination of the kinetics of phosphorylation of the Kv4.2 C-terminus construct by ERK2. The concentration curve for ERK2 phosphorylation of the Kv4.2 C-terminal domain fusion protein is shown. The K_m and V_{max} values were calculated from Lineweaver–Burke plots of these data. The K_m value was estimated to be 60 n*M*, and the V_{max} was determined to be 36 pmol/min/mg.

son et al., 1990), a synthetic peptide corresponding to the phosphorylation domain of Kv4.2 (residues 598–619) was a poor ERK2 substrate in vitro (data not shown).

Sites of MAPK phosphorylation in the C-terminal domain of the Kv4.2 channel

To determine the sites at which ERK2 can phosphorylate the C-terminal domain of Kv4.2, we first phosphorylated the C-terminus fusion construct in vitro. Following an enzymatic digestion, the resulting phosphopeptides were separated by reverse-phase HPLC (Fig. 3A, upper panel). Fractions 72, 73, 77, 78, 79, 80, 84, and 85, which contained high levels of radioactivity, were pooled for sequencing (Fig. 3A, lower panel). The sequencing results revealed that a single phosphorylated peptide was contained in all the phosphopeptide-containing fractions; this peptide corresponded to amino acids 586–618 of the C-terminus of Kv4.2. We determined the sites of phosphorylation to be threonines at positions 602 and 607 and a serine at position 616 (Fig. 3B, upper panel). Thr^{607} and Ser^{616} were phosphorylated roughly equally; Thr^{602} showed less phosphorylation relative to the other two amino acids (Fig. 3B, lower panel). All three of these

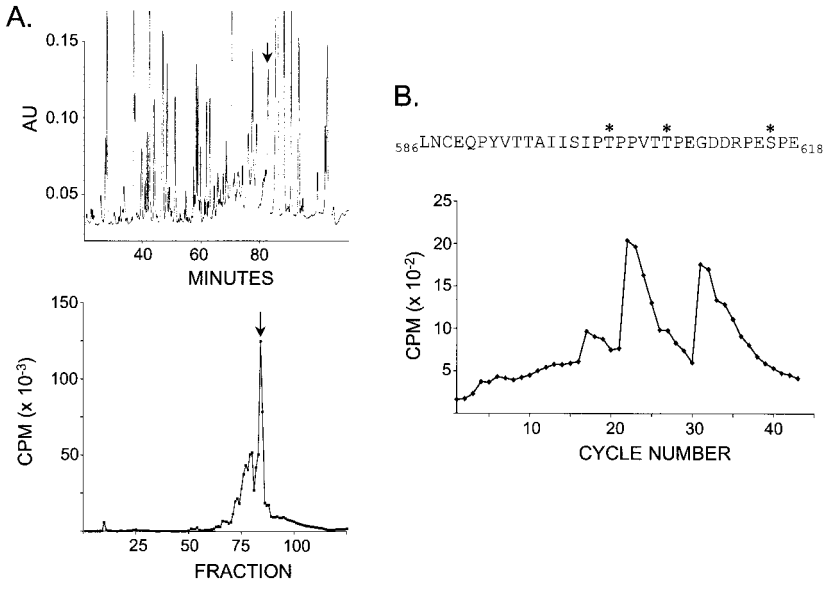

FIG. 3. Sites of ERK2 phosphorylation of Kv4.2. **A: Upper panel:** The absorption at 214 nm (AU = absorbance units) for the phosphorylated C-terminal domain after digestion with Lys-C and separation by reverse-phase HPLC. Fractions were collected starting at min 20; thereafter, fractions were collected every 45 s. A peak is seen in fractions 72, 73, 77–80, 84, and 85 (corresponding to min 74, 74.75, 77.75–80, 83, and 83.75). The peaks indicate the presence of a peptide in these fractions. **Lower panel:** CPM were determined for each HPLC fraction. Fractions 84 and 85 showed the highest radioactivity; fractions 72, 73, and 77–80 also had high CPM. **B: Upper panel:** Sequence of the Kv4.2 peptide found in the HPLC fractions that contained high CPM showing the amino acids phosphorylated by ERK2 (indicated by asterisks). Each HPLC fraction was sequenced separately; each contained the same phosphopeptide. **Lower panel:** CPM were determined for each amino acid in the phosphopeptide. Three cycles showed peaks of radioactivity: 17, 22, and 31, corresponding to Thr^{602}, Thr^{607}, and Ser^{616}. The plot of the CPM released for each cycle extends longer than the sequence of the peptide because we were able to monitor ^{32}P release even after the identification of amino acids had fallen below the limit of detection.

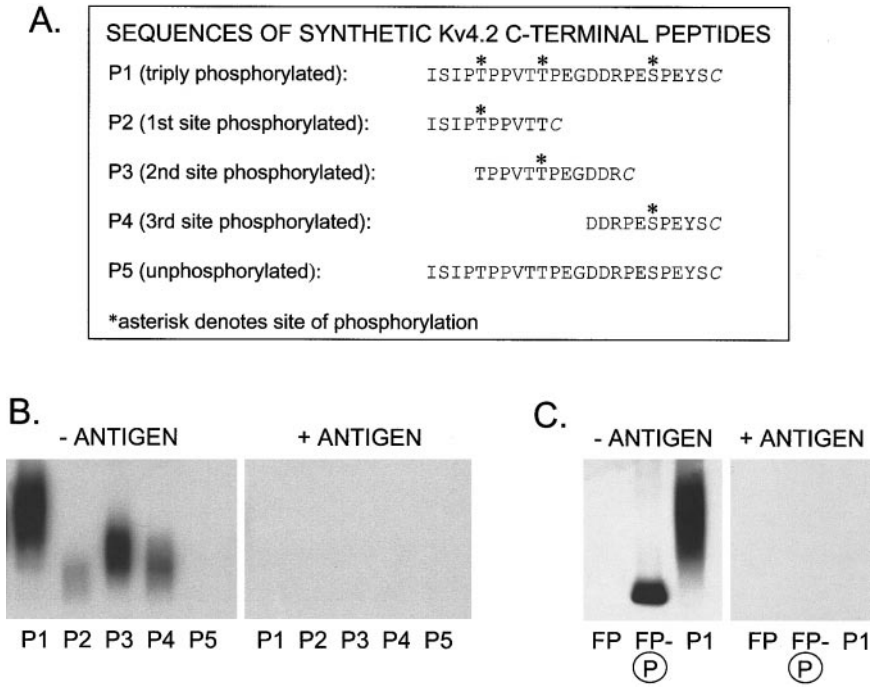

FIG. 4. Development and characterization of the phospho-selective antibody JPA170. **A:** Sequences of the synthetic peptides used as antigens. Peptides 1–4 (P1–P4) were made as phosphopeptides with a cysteine on the C-terminus; the phosphopeptides were coupled to carrier proteins via this cysteine. For antiserum production, the phosphopeptides were coupled to keyhole limpet hemocyanin; after coupling, the antigens were injected into rabbits. Peptide 5 (P5) was not used as an antigen. **B:** Western blot of peptides 1–5. Lanes 1–5 on each blot show peptides 1–5 coupled to ovalbumin. The left blot is probed with the purified version of the antibody made against the triply phosphorylated peptide P1 (antibody JPA170), whereas the right blot is probed with antibody JPA170 preincubated with P1. The molecular heterogeneity of the coupling of ovalbumin to the peptide likely causes the coupled peptide to be recognized by the antibody as a smear. Antibody JPA170 showed highest levels of immunoreactivity against its own peptide, with less immunoreactivity against the single phosphorylation site peptides. The antibody shows no appreciable levels of immunoreactivity against the unphosphorylated peptide. All immunoreactivity is blocked when the antibody is preincubated with antigen. **C:** Western blots of the GST-C-terminus fusion protein. Lane 1, GST-C-terminus fusion protein; lane 2, GST-C-terminus fusion protein incubated with activated ERK2; lane 3, P1. The left blot is probed with antibody JPA170, whereas the right blot is probed with antibody JPA170 preincubated with P1. Antibody JPA170 shows increased levels of immunoreactivity against the phosphorylated fusion protein compared with the unphosphorylated fusion protein, demonstrating appreciable phospho-selectivity. All immunoreactivity is blocked by preincubation of the antibody with antigen.

sites conform to the minimal MAPK consensus site: a serine or threonine directly followed by a proline.

Phospho-antibody production and characterization

To be able to determine if ERK phosphorylates the native channel at the sites identified in vitro, we generated phospho-site-selective antisera. Five synthetic peptides were produced (Fig. 4A): P1 contained phosphate groups attached to Thr^{602}, Thr^{607}, and Ser^{616}; P2, P3, and P4 contained a phosphate group attached to only one of the sites; P5 contained no attached phosphate groups. Antisera against the four phosphopeptides were produced in rabbits. After a terminal bleed was taken, the antisera were purified using affinity columns containing the appropriate phosphopeptide. The purified antibodies (JPA170, JPA172, JPA174, and JPA177) were subsequently characterized.

As a first step in the characterization of the antibodies, we used western blot techniques to test the immunoreactivity of the antibodies against their corresponding peptides. The western blot results show that the antibody generated against the triply phosphorylated peptide, JPA170, is specific for the phosphopeptide it was made against (Fig. 4B). In addition to the recognition of its own peptide, antibody JPA170 also exhibited immunoreactivity against the singly phosphorylated peptides. Conversely, antibody JPA170 showed no immunoreactivity against the unphosphorylated peptide P5. These results indicate that antibody JPA170 is selective for the channel peptides in a phosphorylated state. The antibodies generated against the singly phosphorylated peptides showed similar results using western blot techniques. We found that each of these antibodies was selective for the peptide against which it was made, and was not selective for the unphosphorylated peptide (data not shown).

As a second step in the characterization of the antibodies, we tested the immunoreactivity of the antibodies against the GST-C-terminus fusion protein. Western blotting with antibody JPA170 demonstrated selective detection of the fusion protein incubated with activated ERK2, compared with the unphosphorylated fusion protein (Fig. 4C). Although we will focus on the use of antibody JPA170 for the remainder of the article, it should be noted that similar results were found with antibodies JPA172, JPA174, and JPA177 at this step in the characterization of the antibodies (data not shown). These results confirm that the antibodies are selective for phosphorylated forms of the channel peptides. In addition, these results serve as an internal control for the initial experiments in which we investigated the ability of the C-terminal domain of Kv4.2 to act as a substrate for MAPK in vitro, as well as serving as an independent confirmation of the experiments in which we determined the individual phosphorylation sites on the C-terminal domain of Kv4.2.

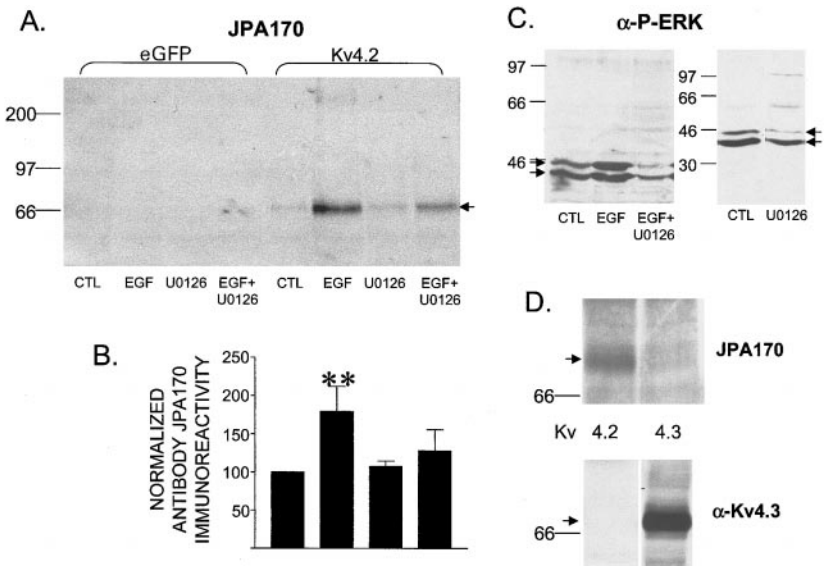

FIG. 5. Antibody JPA170 detects modulation of full-length Kv4.2 phosphorylated by ERK in the intact cell. **A:** Representative western blots of COS-7 cells transfected with enhanced green fluorescent protein (eGFP) or full-length Kv4.2 and probed with antibody JPA170. For each blot: lane 1, cells treated with vehicle (CTL); lane 2, cells stimulated with 10 μM EGF (EGF); lane 3, cells treated with 20 μM U0126 (U0126); lane 4, cells treated with EGF in conjunction with U0126 (EGF + U0126). In the eGFP-transfected cells, no immunoreactivity is seen when probed with antibody JPA170. The appropriate molecular mass of Kv4.2 is indicated with an arrow. **B:** Summary of densitometric analysis of lanes 5–8 in A. Stimulation of the cells with 10 μM EGF led to increased phosphorylation of Kv4.2 by ERK as detected with antibody JPA170 (178.97 ± 33.02% of control, n = 8, $p < 0.01$; ANOVA, followed by Tukey's multiple comparison test). This increase in immunoreactivity is returned toward basal levels with conjunctive application of EGF and the MEK inhibitor U0126 (127.77 ± 27.65% of control, n = 8). In this cell expression system, U0126 does not appear to have a significant effect on basal JPA170 immunoreactivity (107.31 ± 7.07% of control, n = 7). **C:** Representative western blots of COS-7 cells transfected with full-length Kv4.2 and probed with an antibody that recognizes activated, phosphorylated ERK1/2 (α-P-ERK). α-P-ERK recognizes both the p44 (ERK1) and the p42 (ERK2) isoforms of ERK, which are indicated with arrows. For left blot: lane 1, cells treated with vehicle (CTL); lane 2, cells stimulated with 10 μM EGF (EGF); lane 3, cells treated with EGF in conjunction with U0126 (EGF + U0126). For right blot: lane 1, cells treated with vehicle (CTL); lane 2, cells treated with 20 μM U0126 (U0126). α-P-ERK shows increased immunoreactivity when the cells are stimulated with EGF; this immunoreactivity is decreased below basal levels with conjunctive application of EGF and U0126. **D:** Western blots of COS-7 cells transfected with Kv4.2 (lane 1) or Kv4.3 (lane 2). The top blot is probed with antibody JPA170, whereas the bottom blot is probed with an anti-Kv4.3 antibody. The appropriate molecular mass of Kv4.2 is indicated with an arrow. Antibody JPA170 shows significant immunoreactivity of Kv4.2, but not Kv4.3. The anti-Kv4.3 antibody shows the opposite result. These results indicate that antibody JPA170 does not cross-react with Kv4.3, a similar A-type K^+ channel found in the hippocampus.

The phospho-site-selective antibody JPA170 recognizes Kv4.2 in the intact cell

To ascertain if channels formed by Kv4.2 subunits can be phosphorylated by ERK, we examined the ability of antibody JPA170 to recognize Kv4.2 in the intact cell. In western blotting experiments using antibody JPA170, cells transfected with a control construct showed no immunoreactivity at the appropriate band (Fig. 5A, left side of blot), whereas cells expressing the full-length Kv4.2 channel showed a basal level of immunoreactivity to a band migrating at 70 kDa, the estimated molecular mass of one subunit of Kv4.2 (Fig. 5A, right side of blot). Treating cells expressing Kv4.2 with 10 μM epidermal growth factor (EGF; 10-min incubation) resulted in significantly increased immunoreactivity against antibody JPA170 (178.97 ± 33.02% of control, n = 8, $p < 0.01$; Fig. 5A and B), as well as an antibody that recognizes phosphorylated, activated ERK (α-P-ERK; Fig. 5C, left blot). This immunoreactivity was attenuated upon incubation of the cells with 20 μM U0126 in conjunction with EGF (127.77 ± 27.65% of control, n = 8, Fig. 5A and B; Fig. 5C, right blot). It should be noted that at the time point tested, U0126 did not have a significant effect on basal phosphorylation of Kv4.2 by ERK. This lack of an effect could be due to slow turnover of phosphorylation. These data demonstrate that antibody JPA170 can detect a basal level of ERK phosphorylation of the full-length Kv4.2 channel in an intact cell; furthermore, the antibody can detect modulation of this phosphorylation. These data establish that Kv4.2 is an ERK substrate subject to phosphorylation in the living cell.

We also used the COS-7 cell expression system to examine the cross-reactivity of JPA170 with a similar A-type channel, Kv4.3. Kv4.3 shares 71% identity with Kv4.2 and exhibits similar localization patterns. However, although the two channels are often found in the same brain region, their expression does not necessarily overlap (Barry et al., 1995; Serodio et al., 1996; Serodio and Rudy, 1998). For instance, in situ hybridization studies show mRNA labeling of Kv4.2 in hippocampal area CA1, CA3, and dentate gyrus; in contrast, Kv4.3 mRNA is labeled only in area CA3 and dentate gyrus. In our experiments, Kv4.2 or Kv4.3 cDNA was transfected into COS-7 cells. In western blots of cell homogenates probed with antibody JPA170, no immunoreactivity was seen against Kv4.3. Similar western blots with an anti-Kv4.3 antibody revealed significant immunoreactivity against Kv4.3 (Fig. 5C), confirming adequate expression levels of Kv4.3. These results indicate that antibody JPA170 can be used to reliably examine the phosphorylation of Kv4.2 in tissues that express both Kv4.2 and Kv4.3. It should be noted that another Kv4 channel, Kv4.1, exists. However, it has been reported that this channel is not abundantly expressed in either the heart or brain (Dixon and McKinnon, 1994; Serodio et al., 1996).

Kv4.2 phosphorylated by ERK is present in rat hippocampus

We next examined the phosphorylation state of Kv4.2 in rat hippocampus using the phospho-selective antibody JPA170. In western blot experiments with preparations of area CA1 microdissected from transverse hippocampal slices, antibody JPA170 showed immunoreactivity against an appropriately migrating band (Fig. 6A). In addition, this band migrates at the same molecular weight as a band detected with an antibody that recognizes the C-terminus of Kv4.2 (α-Kv4.2; Fig. 6C). In these experiments, application of 10 or 20 μM U0126 to the hippocampal slices for 1 h led to a decrease in immunoreactivity using antibody JPA170 (61.13 $\pm$ 7.69% of control, n = 17, $p < 0.005$; Fig. 6B), indicating that manipulating ERK activity in the hippocampus results in altered Kv4.2 phosphorylation. In addition, the results from these experiments establish that in hippocampal area CA1, antibody JPA170 can be used to detect native, ERK-phosphorylated Kv4.2.

To examine the subcellular pattern of phosphorylation of Kv4.2 by ERK, we used antibody JPA170 in immunohistochemical experiments (see Fig. 6D). In these experiments, adult mouse brains were removed, frozen, and mounted for cryostat sectioning. Twenty-micrometer sections were processed using antibody JPA170 as the primary antibody. Staining was revealed with metal-enhanced diaminobenzidine. The pattern of hippocampal staining was found to be similar to that reported for total Kv4.2 in rat (Sheng et al., 1992), and is in good agreement with the hippocampal staining pattern for phospho-ERK found in the rat (Bhat et al., 1998; Flood et al., 1998). We found that in area CA1, staining was high in stratum oriens and stratum radiatum, light in stratum lacunosum molecular, and absent in stratum pyramidale. In area CA3, immunoreactivity was high in stratum oriens and stratum pyramidale, but absent in stratum lucidum. In the dentate gyrus, staining was low in the molecular layer and the granule cell layer. This pattern of staining indicates that Kv4.2 phosphorylated by ERK is present in both the apical and basilar dendrites of the pyramidal cells of area CA1, but not the pyramidal cell bodies themselves. In area CA3, staining is present in the cell bodies and the basilar dendrites, but not the dendrites receiving information from the dentate gyrus. Correspondingly, low staining was seen in the cell bodies or dendrites of the dentate gyrus. These results demonstrate that antibody JPA170 can be used in immunohistochemical procedures to examine the localization of Kv4.2 phosphorylated by ERK. These data also reveal an interesting input-specific labeling pattern of phospho-Kv4.2 in the hippocampus.

DISCUSSION

In this study, we determined that the A-type K^+ channel Kv4.2 is a substrate for ERK, and we developed a tool with which to study the phosphorylation of Kv4.2 by ERK. Similar to the approach used by Anderson et al. (2000) to identify PKA phosphorylation sites on Kv4.2, we first used recombinant Kv4.2 proteins to determine that the C-terminus, but not the N-terminus, of Kv4.2 is an effective substrate for ERK2. Direct amino acid sequencing of the phosphorylated C-terminal domain revealed that three amino acids are phosphorylated by ERK2: Thr^{602}, Thr^{607}, and Ser^{616}.

To be able to detect the phosphorylation of Kv4.2 by ERK in the hippocampus, we developed an antibody (JPA170) that recognizes Kv4.2 phosphorylated by ERK at the sites identified in vitro. Characterization of this antibody revealed that it is phospho-selective and can detect modulation of the phosphorylation state of full-length Kv4.2 expressed in intact cells. One interesting finding that arose from these studies was the growth factor-induced increase in immunoreactivity seen with antibody JPA170. EGF has long been known to activate the ERK cascade in mitotic cells and has been found recently to activate the ERK cascade in postmitotic cells (Yamada et al., 1997). Our results suggest that growth factors may be linked to the regulation of membrane excitability through ERK phosphorylation of a K^+ channel.

We also used antibody JPA170 to detect not only the native channel phosphorylated by ERK in hippocampal area CA1, but also an alteration of the phosphorylation of Kv4.2 in area CA1. Thus, we now have a tool with which to examine the regulation of the phosphorylation of the A-type K^+ channel Kv4.2 by ERK in the hippocampus during synaptic plasticity. For instance, this antibody could be used to investigate changes in the phosphorylation of Kv4.2 by ERK during LTP, epilepsy, development, and neurodegenerative disorders.

FIG. 6. Antibody JPA170 detects native Kv4.2 phosphorylated by ERK in hippocampal area CA1. **A:** Representative western blot of hippocampal area CA1 tissue probed with antibody JPA170. The transverse hippocampal slices were treated with vehicle (control) or the MEK inhibitor U0126 (10 or 20 μM). The position of native Kv4.2 is marked with an arrow. **B:** Summary of densitometric analysis. Incubation with U0126 decreased the immunoreactivity of antibody JPA170 relative to control. Control = 100%, n = 17; U0126 = 61.13 $\pm$ 7.69% of control, n = 17; $p < 0.005$, Student's *t* test. **C:** Representative western blot of hippocampal area CA1 tissue probed with an antibody that recognizes total Kv4.2 (α-Kv4.2). The position of native Kv4.2 is marked with an arrow. The band detected with this antibody migrates at the same place as the band detected with antibody JPA170. **D:** Immunohistochemical staining of mouse hippocampus using antibody JPA170. The sections are shown at $\times$40. The top section is probed with antibody JPA170; the bottom section is probed with antibody JPA170 preincubated with antigen (P1). In hippocampal area CA1 of this section, staining is intense in stratum oriens (so) and stratum radiatum (sr), but is minimal in stratum pyramidale (sp); staining is also present in stratum lacunosum-moleculare (slm). In area CA3, staining is intense in stratum pyramidale and stratum oriens, but is low in stratum lucidum (sl). No areas of the dentate gyrus (DG) were appreciably stained [molecular layer (ml-dg); granule layer (gl-dg)].

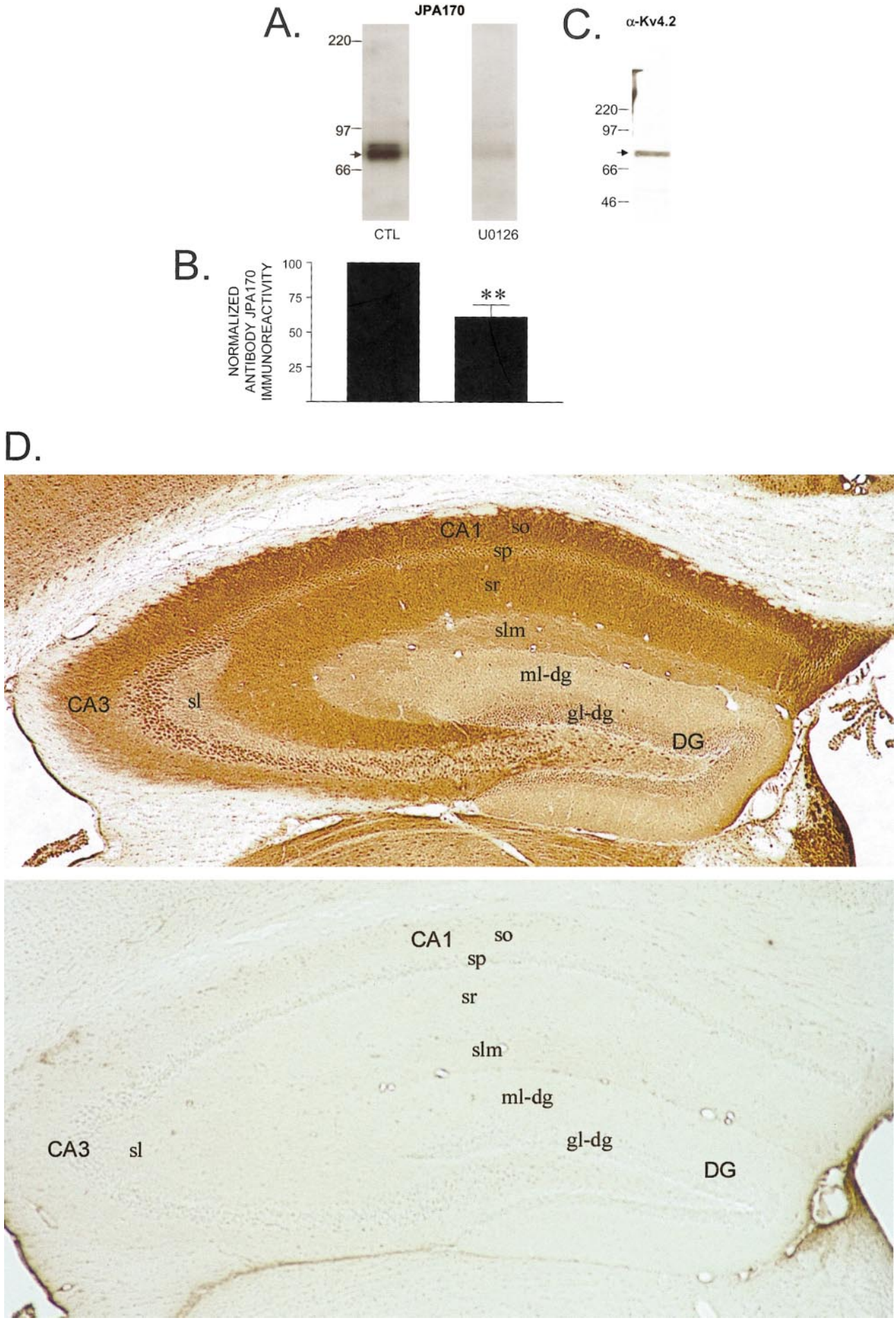
A.
JPA170
220
97
66
CTL
U0126
C.
α-Kv4.2
220
97
66
46
B.
NORMALIZED ANTIBODY JPA170 IMMUNOREACTIVITY
100
75
50
25
**
D.
CA1
so
sp
sr
slm
ml-dg
gl-dg
DG
CA3
sl
CA1
so
sp
sr
slm
ml-dg
gl-dg
DG
CA3
sl

One particularly interesting implication of our work is the potential role of ERK in the regulation of Kv4.2 in LTP. LTP is a voltage-dependent process requiring a transient voltage-dependent inward flux of calcium (Lynch et al., 1983; Malinow and Miller, 1986). Johnston and colleagues (Hoffman et al., 1997; Magee and Johnston, 1997) have proposed a model in which A-type channels in distal dendrites of the hippocampus can coincidentally detect excitatory postsynaptic potentials and back-propagating action potentials. This model proposes that inactivation of A-type channels by the excitatory postsynaptic potential causes an increase in the ability of the back-propagating action potential to invade a particular dendrite. Additional decreases in the ability of the channels to pass current due to phosphorylation could further enhance the possibility of achieving LTP at a particular synapse. It is interesting that Hoffman and Johnston (1998) found that application of activators of PKA or PKC shifted the activation curve of A-type K^+ currents recorded in hippocampal area CA1 dendrites, leading to increases in dendritic excitability. Roberson et al. (1999) have demonstrated that activation of PKA and PKC both lead to ERK activation in CA1 pyramidal neurons, suggesting that the modulation of I_A by PKA or PKC may be due to ERK phosphorylation of Kv4.2. Phosphorylation of the Kv4.2 channel by ERK during LTP induction may lead to increased excitability and membrane depolarization of neurons, which would increase the magnitude of the calcium influx and the probability of triggering LTP.

We have demonstrated here that Kv4.2 is an ERK substrate. The most exciting implication of these data is that ERK may control excitability of pyramidal neurons in the hippocampus. Most studies of plasticity in the hippocampus have focused on synaptic plasticity. Regulation of Kv4.2 by protein kinases opens up the possibility of a higher level of plasticity imposed one step above the synapse, i.e., controlling global cellular excitability. Such suprasynaptic plasticity may play a critical role in controlling the overall information processing properties of neurons in the CNS. The studies described here, along with the new reagents we have developed, generate the potential for studying the basis of this phenomenon at the molecular level.

Acknowledgment: This work was supported by grants from NIMH, NARSAD, NICHD, and NINDS.

REFERENCES

Adams J. P., Selcher J. C., and Sweatt J. D. (1999) U0126: an effective inhibitor of MAPK activation in neuronal tissue. *Neural Notes* **5,** 14–16.

Alonso G. and Widmer H. (1997) Clustering of KV4.2 potassium channels in postsynaptic membrane of rat supraoptic neurons: an ultrastructural study. *Neuroscience* **77,** 617–621.

Anderson A. E., Adams J. P., Qian Y., Cook R. G., Pfaffinger P. J., and Sweatt J. D. (2000) Kv4.2 phosphorylation by cyclic AMP-dependent protein kinase. *J. Biol. Chem.* **275,** 5337–5346.

Atkins C. M., Selcher J. C., Petraitis J. J., Trzaskos J. M., and Sweatt J. D. (1998) The MAPK cascade is required for mammalian associative learning. *Nat. Neurosci.* **1,** 602–609.

Baldwin T. J., Tsaur M.-L., Lopez G. A., Jan Y. N., and Jan L. Y. (1991) Characterization of a mammalian cDNA for an inactivating voltage-sensitive K^+ channel. *Neuron* **7,** 471–483.

Barry D. M., Trimmer J. S., Merlie J. P., and Nerbonne J. M. (1995) Differential expression of voltage-gated K^+ channel subunits in adult rat heart. Relation to functional K^+ channels? *Circ. Res.* **77,** 361–369.

Berman D. E., Hazvi S., Rosenblum K., Seger R., and Dudai Y. (1998) Specific and differential activation of mitogen-activated protein kinase cascades by unfamiliar taste in the insular cortex of the behaving rat. *J. Neurosci.* **18,** 10037–10044.

Bhat R. V., Engber T. M., Finn J. P., Koury E. J., Contreras P. C., Miller M. S., Dionne C. A., and Walton K. M. (1998) Region-specific targets of p42/p44MAPK signaling in rat brain. *J. Neurochem.* **70,** 558–571.

Blum S., Moore A. N., Adams F., and Dash P. K. (1999) A mitogen-activated protein kinase cascade in the CA1/CA2 subfield of the dorsal hippocampus is essential for long-term spatial memory. *J. Neurosci.* **19,** 3535–3544.

Cassell J. F. and McLachlan E. M. (1986) The effect of a transient outward current (I_A) on synaptic potentials in sympathetic ganglion cells of the guinea-pig. *J. Physiol. (Lond.)* **374,** 273–288.

Dineley K. T. and Patrick J. W. (2000) Amino acid determinants of α7 nicotinic acetylcholine receptor surface expression. *J. Biol. Chem.* **275,** 13974–13985.

Dixon J. E. and McKinnon D. (1994) Quantitative analysis of potassium channel mRNA expression in atrial and ventricular muscle of rats. *Circ. Res.* **75,** 252–260.

English J. D. and Sweatt J. D. (1996) Activation of p42 mitogen-activated protein kinase in hippocampal long term potentiation. *J. Biol. Chem.* **271,** 24329–24332.

English J. D. and Sweatt J. D. (1997) A requirement for the mitogen-activated protein kinase cascade in hippocampal long-term potentiation. *J. Biol. Chem.* **272,** 19103–19106.

Erickson A. K., Payne D. M., Martino P. A., Rossomando A. J., Shabanowitz J., Weber M. J., Hunt D. F., and Sturgill T. W. (1990) Identification by mass spectrometry of threonine 97 in bovine myelin basic protein as a specific phosphorylation site for mitogen-activated protein kinase. *J. Biol. Chem.* **265,** 19728–19735.

Fiore R. S., Bayer V. E., Pelech S. L., Posada J., Cooper J. A., and Baraban J. M. (1993) p42 mitogen-activated protein kinase in brain: prominent localization in neuronal cell bodies and dendrites. *Neuroscience* **55,** 463–472.

Flood D. G., Finn J. P., Walton K. M., Dionne C. A., Contreras P. C., Miller M. S., and Bhat R. V. (1998) Immunolocalization of the mitogen-activated protein kinases p42MAPK and JNK1, and their regulatory kinases MEK1 and MEK4, in adult rat central nervous system. *J. Comp. Neurol.* **398,** 373–392.

Fredericks Z. L., Pitcher J. A., and Lefkowitz R. J. (1996) Identification of the G protein-coupled receptor kinase phosphorylation sites in the human beta2-adrenergic receptor. *J. Biol. Chem.* **271,** 13796–13803.

Hoffman D. A. and Johnston D. (1998) Downregulation of transient K^+ channels in dendrites of hippocampal CA1 pyramidal neurons by activation of PKA and PKC. *J. Neurosci.* **18,** 3521–3528.

Hoffman D. A., Magee J. C., Colbert C. M., and Johnston D. (1997) K^+ channel regulation of signal propagation in dendrites of hippocampal pyramidal neurons. *Nature* **387,** 869–875.

Impey S., Obrietan K., and Storm D. R. (1999) Making new connections: role of ERK/MAP kinase signaling in neuronal plasticity. *Neuron* **23,** 11–14.

Jonas E. A. and Kaczmarek L. K. (1996) Regulation of potassium channels by protein kinases. *Curr. Opin. Neurobiol.* **6,** 318–323.

Kennelly P. J. and Krebs E. G. (1991) Consensus sequences as substrate specificity determinants for protein kinases and protein phosphatases. *J. Biol. Chem.* **266,** 15555–15558.

Lev S., Moreno H., Martinez R., Canoll P., Peles E., Musacchio J. M., Plowman G. D., Rudy B., and Schlessinger J. (1995) Protein tyrosine kinase PYK2 involved in Ca^{2+}-induced regulation of ion channel and MAP kinase functions. *Nature* **376,** 737–745.

Lynch G., Larson J., Kelso S., Barrionuevo G., and Schottler F. (1983) Intracellular injections of EGTA block induction of hippocampal long-term potentiation. *Nature* **305,** 719–721.

Magee J. C. and Johnston D. (1997) A synaptically controlled, associative signal for Hebbian plasticity in hippocampal neurons. *Science* **275,** 209–213.

Maletic-Savatic M., Lenn N. J., and Trimmer J. S. (1995) Differential spatiotemporal expression of K^+ channel polypeptides in rat hippocampal neurons developing *in situ* and *in vitro*. *J. Neurosci.* **15,** 3840–3851.

Malinow R. and Miller J. P. (1986) Postsynaptic hyperpolarization during conditioning reversibly blocks induction of long-term potentiation. *Nature* **320,** 529–530.

Martina M., Schultz J. H., Ehmke H., Monyer H., and Jonas P. (1998) Functional and molecular differences between voltage-gated K^+ channels of fast-spiking interneurons and pyramidal neurons of rat hippocampus. *J. Neurosci.* **18,** 8111–8125.

Roberson E. D., English J. D., Adams J. P., Selcher J. C., Kondratick C., and Sweatt J. D. (1999) The mitogen-activated protein kinase cascade couples PKA and PKC to CREB phosphorylation in area CA1 of hippocampus. *J. Neurosci.* **19,** 4337–4348.

Rosenfeld J., Capdevielle J., Guillemot J. C., and Ferrara P. (1992) In-gel digestion of proteins for internal sequence analysis after one- or two-dimensional gel electrophoresis. *Anal. Biochem.* **203,** 173–179.

Rudy B., Kentros C., and Vega-Saenz de Miera E. (1991) Families of K^+ channel genes in mammals: toward an understanding of the molecular basis of K^+ channel diversity. *Mol. Cell. Neurosci.* **2,** 89–102.

Schafe G. E., Nadel N. V., Sullivan G. M., Harris A., and LeDoux J. E. (1999) Memory consolidation for contextual and auditory fear conditioning is dependent on protein synthesis, PKA, and MAP kinase. *Learn. Mem.* **6,** 97–110.

Schanen N. C. and Landreth G. (1992) Isolation and characterization of microtubule-associated protein 2 (MAP2) kinase from rat brain. *Mol. Brain Res.* **14,** 43–50.

Selcher J. C., Atkins C. M., Trzaskos J. M., Paylor R., and Sweatt J. D. (1999) A necessity for MAP kinase activation in mammalian spatial learning. *Learn. Mem.* **6,** 478–490.

Serodio P. and Rudy B. (1998) Differential expression of Kv4 K^+ channel subunits mediating subthreshold transient K^+ (A-type) currents in rat brain. *J. Neurophysiol.* **79,** 1081–1091.

Serodio P., Kentros C., and Rudy B. (1994) Identification of molecular components of A-type channels activating at subthreshold potentials. *J. Neurophysiol.* **72,** 1516–1529.

Serodio P., Vega-Saenz de Miera E., and Rudy B. (1996) Cloning of a novel component of A-type K^+ channels operating at subthreshold potentials with unique expression in heart and brain. *J. Neurophysiol.* **75,** 2174–2179.

Sheng M., Tsaur M.-L., Jan Y. N., and Jan L. Y. (1992) Subcellular segregation of two A-type K^+ channel proteins in rat central neurons. *Neuron* **9,** 271–284.

Sweet M. T., Carlson G., Cook R. G., Nelson D., and Allis C. D. (1997) Phosphorylation of linker histones by a protein kinase A-like activity in mitotic nuclei. *J. Biol. Chem.* **272,** 916–923.

Yamada M., Ikeuchi T., and Hatanaka H. (1997) The neurotrophic action and signalling of epidermal growth factor. *Prog. Neurobiol.* **51,** 19–37.